Hindawi
Geofluids
Volume 2022, Article ID 6943834, 10 pages
https://doi.org/10.1155/2022/6943834

Research Article

Effect Of Open-Pit Blasting Vibrations on a Hanging-Wall Slope: A Case Study of the Beizhan Iron Mine in China

Yong-gang Xiao,[1,2] **Jie Cao**,[3] **Xiao-min Liu**,[1] **and Chang-hong Li**[2]

[1]*China Construction Sixth Engineering Division Co. Ltd., Tianjin 300012, China*
[2]*School of Civil and Resource Engineering, University of Science and Technology Beijing, Beijing 100083, China*
[3]*Hebei Petroleum University of Technology, Chengde 067000, China*

Correspondence should be addressed to Jie Cao; caojieshiyou@163.com and Xiao-min Liu; 286237078@qq.com

Received 4 November 2021; Accepted 24 February 2022; Published 17 March 2022

Academic Editor: Yong-Zheng Wu

With the increase in the depth of large-scale open-pit mining, many mines have to face problems such as what is the effect of open-pit blasting on the rock slope and how to ensure the stability of a high-steep slope. The east slope of the Beizhan iron mine in Hejing County, Xinjiang, belongs to the typical open-pit high and steep slope of mined hanging-wall ore. To study the effect of open-pit blasting vibrations on hanging-wall slope stability, the intelligent blasting vibration detector was used to monitor the open-pit blasting wave of the Beizhan iron mine and the corresponding numerical model was established. We fitted the transmission law of slope blasting vibration by Sodev's regression formula and calculated stress, strain, and vibration velocity of the whole slope by numerical simulation. The result showed that the fitting functional relationship was correct and could be the basic rule of predicting the maximum charge amount per delay interval and minimum safe distance for this area. The estimated open-pit blasting charge weight was reasonable and blasting vibrations would have little effect on the hanging-wall slope. The research method and conclusions in this article have numerous reference values for studying the hanging-wall slope's kinetic stability.

1. Introduction

With the quickened pace of large-scale open-pit mining and open-pit mining depth increasing, more and more high-steep slopes are formed. Most mine slopes face problems such as the impact of open-pit blasting on hanging-wall ores and how to ensure the stability of high-steep slopes [1–3]. The hanging-wall ore is part of the ore body extending outside the open-pit boundary [4]. Large-scale blasting during open-pit mining caused great stress disturbance to the surrounding rock mass and stress concentration formed at the bottom of a pit and the foot of a slope. When the hanging-wall ore is mined, a more complex secondary stress field will be formed, causing further deformation and destruction of the surrounding rock of the slope and even engineering disasters such as landslides.

Given the influence of open-pit blasting on high and steep slopes, the commonly used research methods are blasting vibration tests and numerical simulation. The effect of controlled blasting on the stability of mine slopes was studied by Singh et al. [5] through presplit blasting tests. Hu et al. [6] analyzed the correlation between blasting damage depth and peak particle velocity and proposed a new damage-vibration coupling control method for high rock slopes. Yin et al. [7] and others monitored blasting vibration signals using different rock blasting scenes and studied the attenuation characteristic of blasting vibration waves transmitted in the joint rock slope. Rajmeny and Shrimali [8] monitored the sliding of the hanging wall caused by multiple blasting and fitted predictive equations for blast vibration at the Rampura Agucha Mine. Tao et al. [9] used remote monitoring and early warning system to continuously monitor a slope. The monitoring results showed that the open-pit mining technology of a "mechanical gun" instead of "blasting" had effectively reduced the impact of mining disturbance on the stability of the western slope. Bao and others [10]

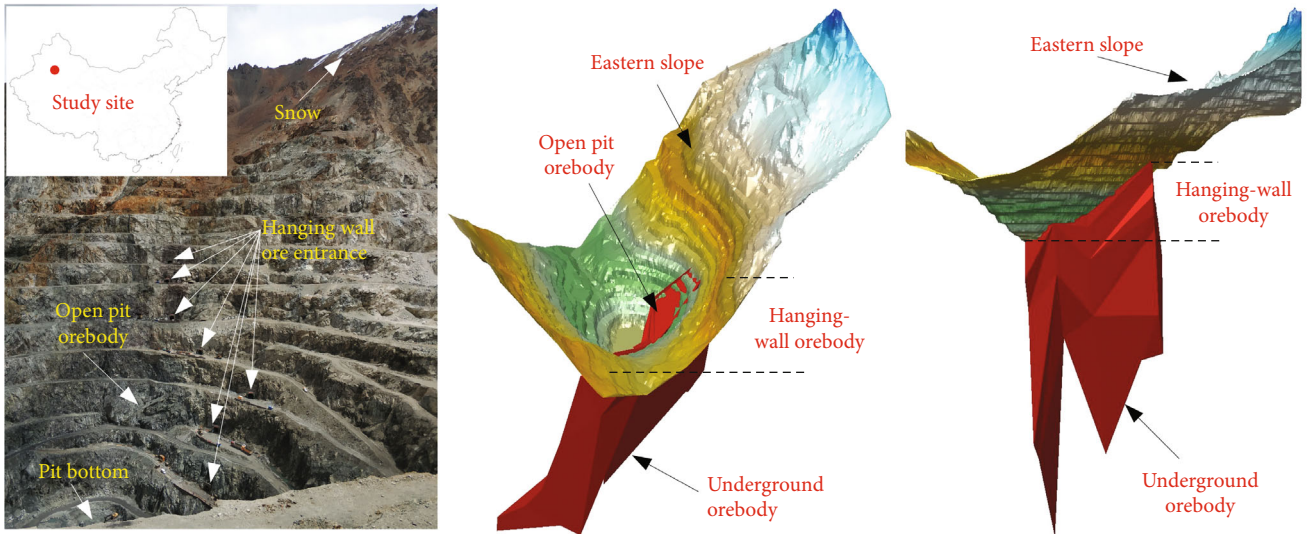

Figure 1: The morphological characteristics of the eastern slope with hanging-wall orebody.

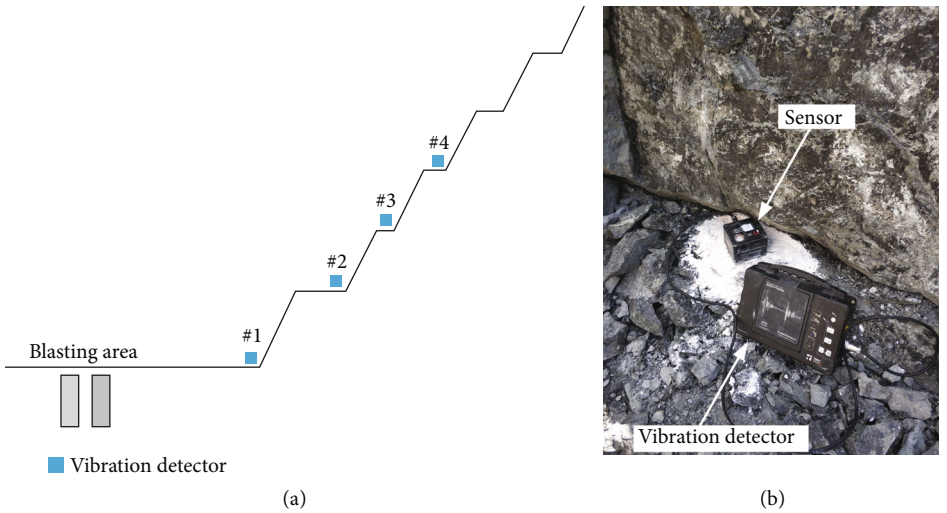

Figure 2: Schematic diagram of the relative positions of the vibration detector installation (a) and the field-installed vibration detector (b).

monitored an open-pit mine using a blasting vibration instrument and they found that the main influencing factors for slope stability were vibration velocity and duration. Xie et al. [11] monitored an open-pit mine slope using a blasting vibration system, and they found that changing the blasting order and direction could reduce blasting vibrations. Ma et al. [12] proved that presplitting blasting played a major role in absorbing blasting shock waves based on the blasting vibration testing of an open-pit mine slope. The numerical simulation analysis method is a common tool to solve mining rock mechanics problems. Hu et al. [13] proposed the relationship between peak vibration velocity and soil properties based on the improved Sodev equation. The classical Sodev empirical formula was improved by Ma et al. [14] to predict the vibration velocity of pipe explosions. A linear fitting model based on Sodev's empirical formula was developed, and blast vibration data from lighthouses near the blast area were monitored by Gu et al. [15]. Researchers used numerical simulation programs such as the finite element method (FEM) [16–22], discrete element method (DEM) [23–27], and finite difference method (FDM) [28–32] to study the dynamic response characteristics of blasting vibration to high and steep slopes. These response characteristics mainly included vibration velocity, displacement, amplification factor, frequency, stress, and strain of slope after blasting. Hu et al. used LS-DYNA software to study the effect of smooth blasting and presplitting blasting on rock high-slope damage and analyzed the spatial distribution of blasting damage [16, 33, 34]. Jiang et al. [35] used blasting excavation of Beijing Metro Line 16 as an example to monitor blasting vibration in the field. A three-dimensional numerical model was established to analyze the response

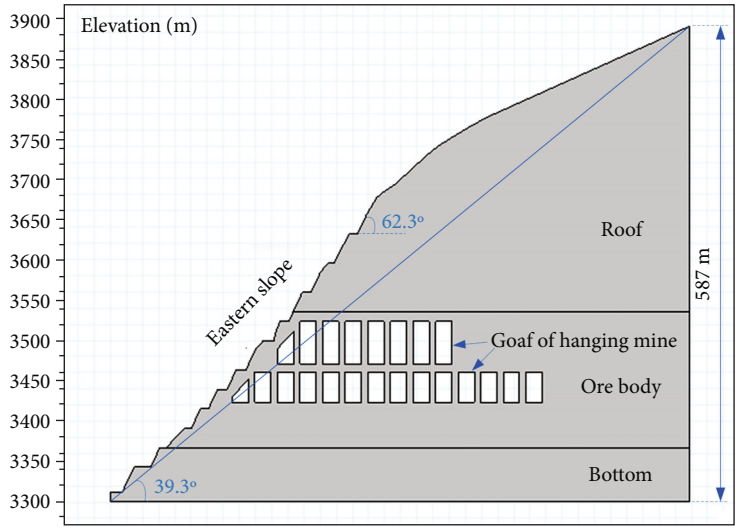

Figure 3: Numerical model of the slope with the hanging-wall ore slope.

Table 1: Statistic of the test results of physical and mechanical properties of rock strata.

Rock layer	Unit weight (kN/m^3)	Elasticity modulus (GPa)	Poisson's ratio	Cohesion (MPa)	Internal friction angle (°)
Roof	25.90	22.5	0.22	11.5	32.02
Orebody	24.80	34.2	0.16	9.8	35.1
Floor	27.10	50	0.17	10.23	31.6

characteristics of buried gas pipelines under the action of blasting vibration. Mohammadi Azizabadi et al. [36] simulated blast seismograms by monitoring single-hole blast vibrations. Then, the particle velocity time histories of blast vibrations in the mine wall were predicted using the universal distinct element code (UDEC). Chen et al. used the tensile-compression damage model to analyze the whole blasting process of the bedding rock slope for numerical simulation. In summary, there were many studies on the influence of open-pit blasting on a rock slope, while there were relatively few studies of the influence of the slope of the mined hanging-wall ore.

The hanging-wall ore mining and open-pit mining are carried out simultaneously in Beizhan's open-pit mine slope of Hejing County, Xinjiang. The mining adit of the hanging-wall mine and platform formed by open-pit mining were combined. The height of the benches was 12 m, and the height of parallel benches was 24 m/36 m. The stripping elevation was 3464 m~3596 m, and the lowest mining elevation was 3390 m. The open-pit benches above 3476 m have been steep. The top-down mining sequence was adopted hanging-wall mining. According to the mining stripping plan, the open-pit production can be continued for about 4 years. With the exploitation of hanging-wall mines and open-pit mines, the mines inside the slope are gradually mined out and the slope gradually becomes higher and steeper. It is necessary to study the influence of open-pit blasting vibration on the slope of the hanging-wall mine.

In this paper, vibration monitoring of Beizhan's open-pit mine slope was carried out by using NUBOX-6016 intelligent vibration monitors. According to the measured blasting vibration wave data, the propagation law of blasting seismic waves on high and steep slopes was studied. Then, the numerical model of the eastern slope of the Beizhan iron mine was established and the measured velocity time-history load at the bottom of the slope was input. Finally, the dynamic response characteristics such as stress, strain, and vibration velocity of high and steep slopes under open-pit blasting vibration were analyzed.

2. Methods

2.1. Geological Overview. The Beizhan iron mine is located in the northwest of Hejing County and the straight-line distance is about 130 km. It is 82 km from Baluntai town, Hejing County, and is under Bayingolin Mongol Autonomous Prefecture, Hejing County's jurisdiction. The mining area is located on the south slope of Yilianhabierga Mountain and west Tianshan Mountain which is a medium-high mountain area. The run of the mountain is nearly an east-west direction and the overall terrain is high in the southern part and low in the north part. The altitude is 3160–4575 m, relative altitude is 700–1000 m, general terrain slope is 25–35°. The ditch is deep and steep. It is a deep alpine landform. The altitude of the part where the orebody is located is 3450–3723 m. A few hundred meters south of the mine site is the ridge of Tianshan Mountain. With the continuous development of open-pit slope mining and under the action of slope excavation and frequent production blasting, the mining area in the south slope had suffered from different degrees of landslides. Especially after the double-step parallel mining, the single-step height reached 36 m, which was prone to instability. The strata in the mining area are mainly the Lower Carboniferous Dahalajunshan Formation, Akshake Formation, and Quaternary. The minimum mining elevation of the open-pit design is 3320 m. It has been mined to an elevation of 3390 meters, and open-pit mining is

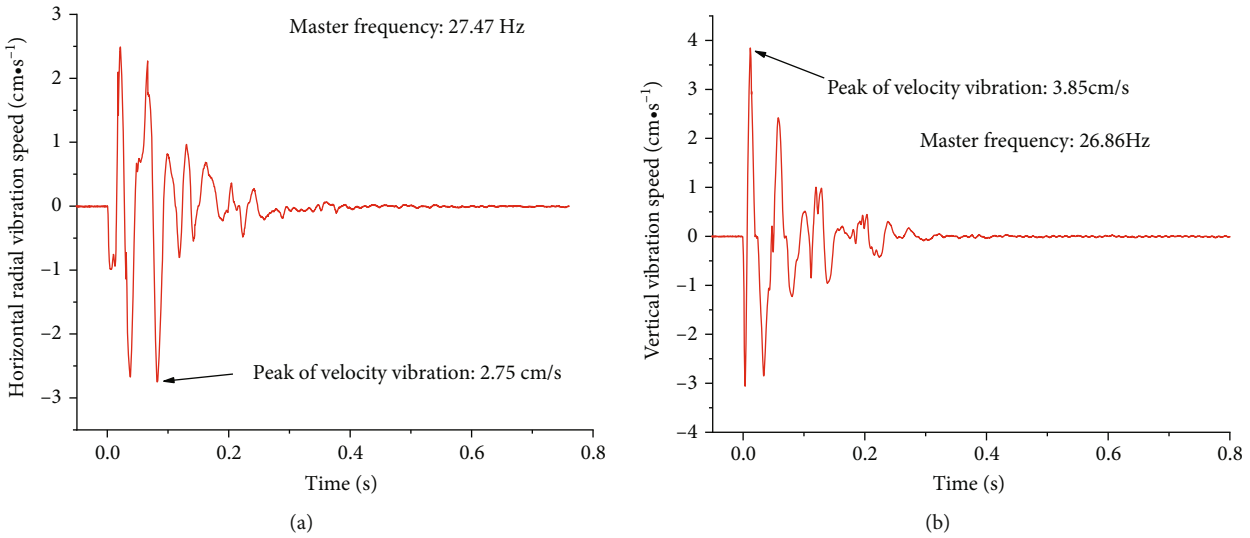

Figure 4: Velocity time history curves of no.1 measuring point in the open-pit blasting. (a) Horizontal radial and (b) vertical.

Table 2: The results of blast vibration monitoring.

Serial number	Maximum charge (kg)	Distance from the explosive center (m)	Horizontal radial		Horizontal tangent		Vertical		Combined vibration velocity (mm/s)
			Vibration velocity (mm/s)	Main frequency (Hz)	Vibration velocity (mm/s)	Main frequency (Hz)	Vibration velocity (mm/s)	Main frequency (Hz)	
1#	480	62	27.49	27.466	35.24	29.297	38.45	26.855	58.96
2#	480	84	41.41	21.362	14.96	28.076	32.15	19.531	54.52
3#	480	92	31.52	62.046	35.28	53.711	3.93	69.289	47.47
4#	480	121	12.87	26.855	0.27	35.368	1.42	52.472	12.95
5#	415	52	24.75	35.753	31.28	41.384	32.76	31.952	51.62
6#	415	79	18.83	31.928	27.86	48.358	25.83	38.261	42.40
7#	415	81	13.87	73.216	16.23	63.893	18.68	83.428	28.37
8#	415	159	10.28	52.467	0.83	83.138	2.73	121.438	10.67
9#	356	55	28.27	29.357	21.63	52.348	30.14	39.271	46.65
10#	356	88	23.64	36.339	19.27	45,773	27.44	38.621	41.03
11#	356	136	11.84	24.414	0.23	37.348	1.83	25.472	11.98
12#	356	152	7.47	14.038	2.27	12.817	1.97	14.038	8.05

coming to an end. In order to maintain the normal production of the mine and ensure the smooth transition from open-pit mining to underground mining, the hanging-wall ore is currently being mined. The present situation of open-pit slope mining and the morphological characteristics of hanging-wall ore are shown in Figure 1.

2.2. Blasting Vibration Test. The blasting area was located at the 3380 elevation mining area on the eastern slope of the pit. This blasting was for progressive mining down to a 3368 elevation. The blasting area was surrounded by buildings of 3404 flat caverns, pumping, and pumping pipes, which were close to the blasting area. The blasting area was all ore. The 3380 m steps were constructed from south to north undercut as required. The main borehole spacing was 2.5 m, the row spacing was 2.0 m, and the inclination angle was 80°. Millisecond delay blasting between rows was adopted in this blasting scheme. Blasting was launched from the west to east row by row in order to achieve the design purpose. The blasting sequence was rowed to row. The way of blasting was reverse initiation. That was, the detonating charge was located at the bottom of the hole and the direction of the energy accumulation hole of the detonator was towards the opening of the hole. The detonating network adopted an electronic-delay detonator. The delay time was set by the electronic detonator and the blasting was carried out from west to east in sections in order to achieve the purpose of blasting in sections and rows.

This test used the NUBOX-6016 intelligent vibration monitor produced by Sichuan Tuopu Measurement and Control Technology Company Ltd. The instrument is connected to a TP3V-4.5 3D velocity-type sensor through a special input signal cable. The first channel of the device is connected to the horizontal x-direction vibration signal,

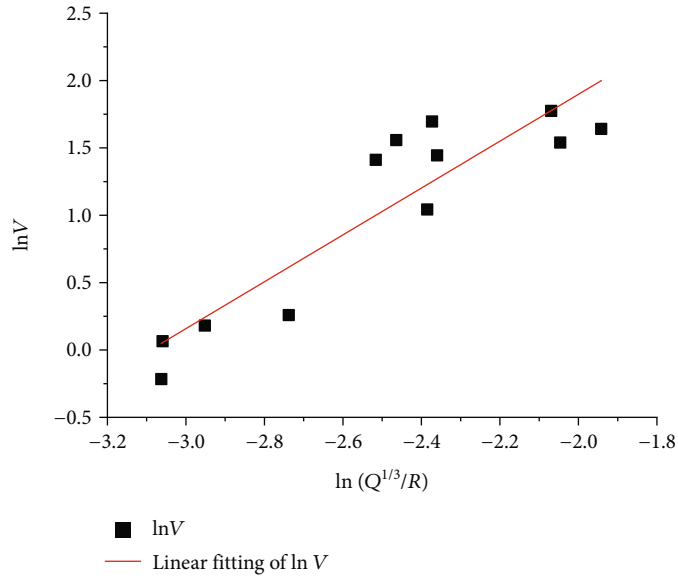

Figure 5: Decay regression line of blasting vibration.

the second channel to the horizontal y-direction signal, and the third channel to the vertical z-direction signal. The TP3V-4.5 three-dimensional velocity sensor is a practical vibration velocity measurement sensor that can simultaneously measure the velocity in the horizontal x, horizontal y, and vertical z directions. The measurement points are located at the foot of the slope. The relative positions of the measurement points and their installation on-site are shown in Figure 2.

2.3. Numerical Simulation of Blasting Vibration. The numerical simulation of blasting vibration would become true by the structural mechanics' module of COMSOL software. The horizontal x-direction and vertical z-direction vibration waves caused by blasting vibration have the greatest influence on the slope stability. Therefore, in the numerical simulation, the x- and z-direction vibration wave signals collected from the test were loaded into the finite element model of the slope at the same time for analysis.

The current slope profile of the hanging-wall ore in the Beizhan iron mine was selected for the study. A numerical model was established according to the shape of the slope and stratigraphic distribution (Figure 3). The model size was 587 m × 716 m, and the maximum step height was 36 m. In order to simulate the near slope blasting, the loading area of the blast load was located on the left boundary of the model, 14 m from the foot of the bottom step. The lithology of the magnetite ore body (layer) in the top and bottom parts is epidote skarn, diopside epidote skarn, tremolite skarn, and tremolite wollastonite skarn, which has great difference in rock integrity. The magnetite massive rock group is mainly composed of brecciated magnetite, disseminated magnetite, and massive magnetite. Its structure is tight, and the joints and fissures are not developed. The ore body has good structural solidity. The statistical values of the physical and mechanical properties of the slope rock test results are shown in Table 1.

This study adopted the low reflection boundary method. The slope surface adopted a free boundary and the rest adopted a low reflection boundary. By default, low reflection boundaries fetch data from adjacent domain materials. The nodes of low reflection boundary let the nonreflection waves flow out with the model to establish a perfect impedance matching for the P wave and S wave. Therefore,

$$\sigma \cdot \mathbf{n} = -\rho c_p \left(\frac{\partial \mathbf{u}}{\partial t} \cdot \mathbf{n}\right)\mathbf{n} - \rho c_s \left(\frac{\partial \mathbf{u}}{\partial t} \cdot \mathbf{t}\right)\mathbf{t}. \quad (1)$$

$\mathbf{n}$ and $\mathbf{t}$ were the unit normal vector and the tangent vector to the boundary, respectively. c_p and c_s were each represented longitudinal wave speed and transverse speed of the material, respectively. This method was most effective when the wave approaches the normal direction of the boundary.

In order to calculate the mechanical characteristics of the slope under different working conditions, three research steps were set up in this study. In the first step, the state of ground stress of the slope before the hanging gang mine was mined was calculated. In the second step, the stress state of the slope after mining was calculated based on the calculation results of the first step. In the third step, the impact of blasting on the slope of the hanging gang mine was calculated based on the first two steps and the response characteristics of the slope to blasting vibration were analyzed.

In general, the vertical and horizontal radial vibration rates have a greater impact on slope stability, while the horizontal tangential rate has a smaller impact on that. In order to avoid large errors in the calculation, this study choses the velocity time history curve that is near the measuring point of the blasting source in the production blasting when calculated as the blasting dynamic load. Only the horizontal radial and vertical vibration rates of this measurement point were selected. The selected time curves of vertical and horizontal radial vibration rates were shown in Figure 4.

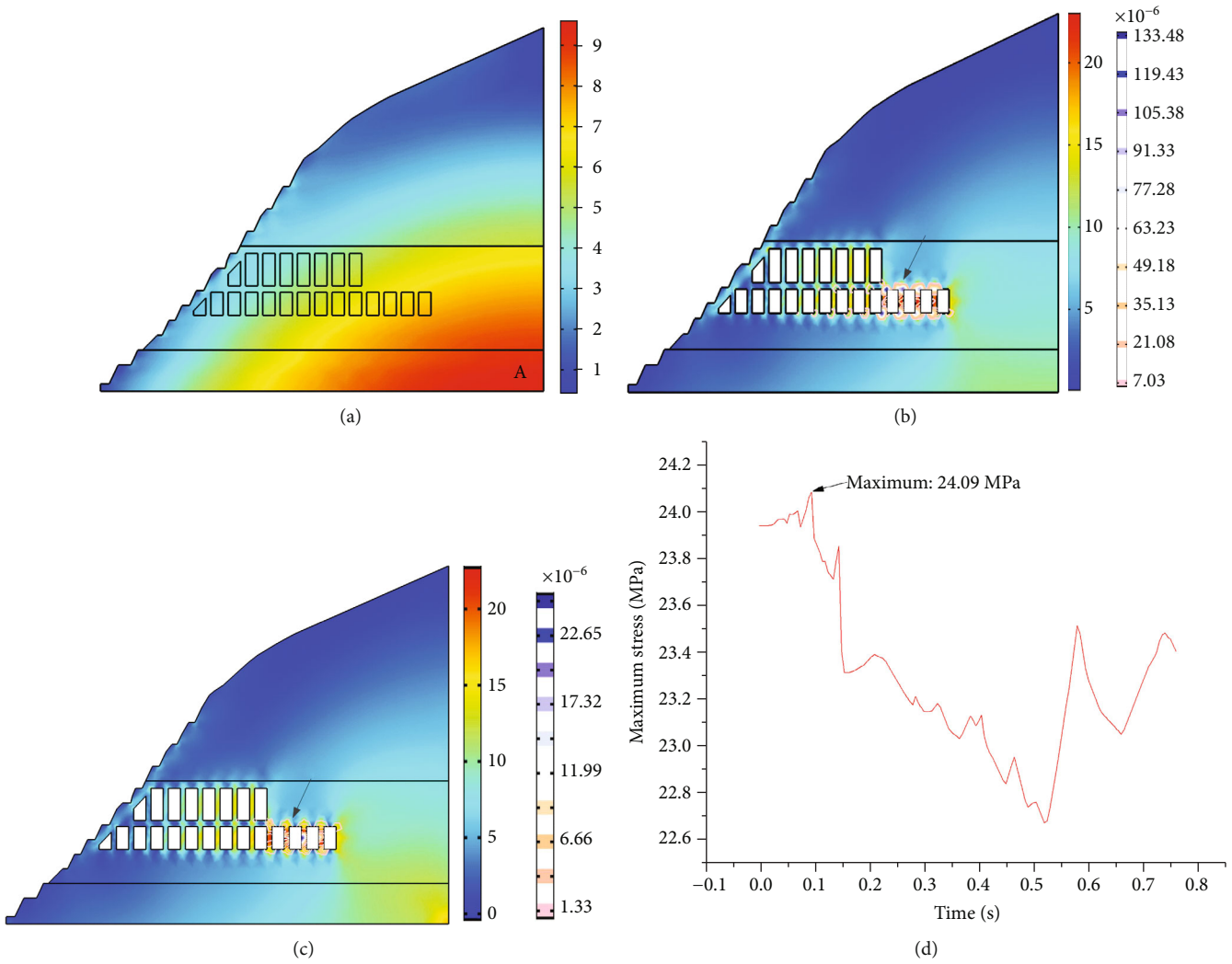

Figure 6: von Mises stress for 3 research steps; (a) before the exploitation of hanging-wall ore; (b) after the exploitation of hanging-wall ore; (c) after open-pit blasting; and (d) maximum stress value's changing law within the slope along with the blasting time.

3. Conclusion and Discussion

3.1. Results and Analysis of Blast Vibration Monitoring. Three blast vibrations in the open pit were monitored using NUBOX-6016 blast vibration detectors. Three monitoring layouts were similar, all along the direction away from the blast source of the 4 monitoring points arranged in turn (Figure 2). The sensor on the monitoring point has the function of monitoring the horizontal radial, horizontal tangential, and vertical direction vibration speed simultaneously. Blast vibration monitoring results are shown in Table 2.

Considering the influence of the maximum charge and the distance from the explosive center on the vibration speed according to *the blasting safety regulations*, the mathematical method of mathematical statistics was used to cope with the measured data by regression analysis. Sodev's regression formula is

$$V = k\left(\frac{Q^{1/3}}{R}\right)^{\alpha}. \quad (2)$$

In the formula, V stands for the maximum 3D synthesis velocity rate of the vibrating particle, cm/s; k and α are coefficients related to the topography and geological conditions between the blasting point and the protected object, respectively; Q is for the maximum single-section charge, kg; R is for the linear distance from the measuring point to the blasting source, m.

A least-mean-square linear regression operation was performed using Sadovsky's formula to fit a straight line (Figure 5). With this, to determine the regression equation, $k = 216.156$, $\alpha = 1.739$, and the correlation coefficient R value was 0.908. This equation can be used as the basis for predicting the maximum single-section charge and minimum safe distance at this site. So, the transmitted law formula of blasting vibration for east slope hanging-wall ore was

$$V = 216.156\left(\frac{Q^{1/3}}{R}\right)^{1.739}. \quad (3)$$

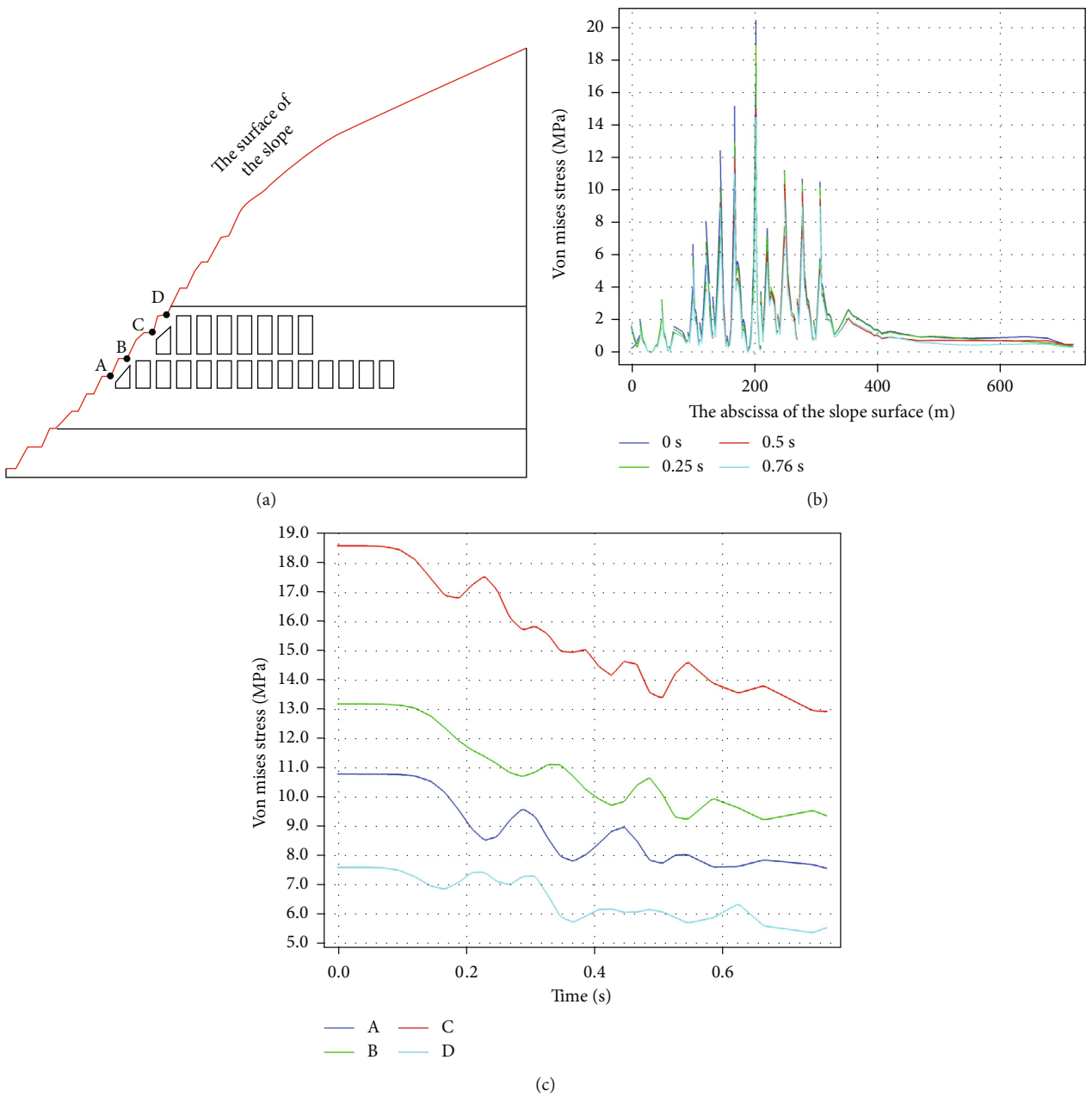

Figure 7: von Mises stress changing situation of the slope and hanging-wall ore mine under blasting vibration: (a) schematic diagram of calculated position of slope and hanging-wall ore mine; (b) von Mises stress changing law of slope surface with different blasting time; (c) von Mises stress changing law of points A, B, C, and D.

The previous experiments could tell that the maximum 3D synthetic velocity of blasting vibration in the toe of the slope was 5.986 cm/s. When the master frequency was greater than 10 Hz and less than 50 Hz according to the *blasting safety regulations*, the safety allowing the velocity range of particle vibration for a permanent rock high steep slope was 8~12 cm/s. The present blasting vibration of the open-pit mine had little impact on slope stability. The slope of the Beizhan iron mine had hanging-wall ore. However, there were no rules for safety allowing the velocity of particle vibration of such slope in *the blasting safety regulations*. Therefore, in order to study the effect of blasting vibration on this slope, a numerical simulation of this slope was established.

3.2. Result and Discussion of Numerical Simulation

3.2.1. Analysis of Stress and Strain. In order to analyze the effect of open-pit blasting on the slope, von Mises stress clouds were obtained from the simulation results before hanging-wall ore mining, after hanging-wall ore mining, and after open-pit blasting (Figure 6). In Figure 6(a), it can be seen that the stresses on the slope before the hanging-wall ore mining were caused by gravity. The

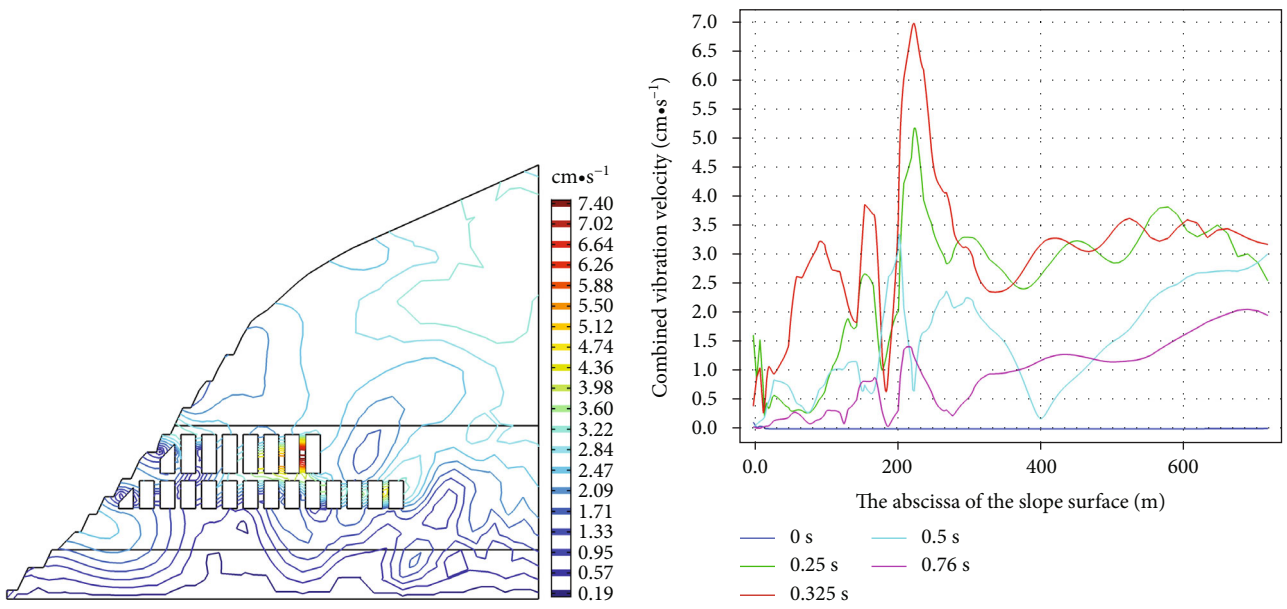

Figure 8: Combined vibration velocity caused by blasting vibration: (a) contour plot of slope combined vibration velocity when $t = 0.265$ s; (b) combined vibration velocity of the surface of the slope.

maximum value was 9.60 MPa in A. There was no plastic strain in the slope. In Figure 6(b), it can be seen that the hanging-wall ore mining caused the redistribution of internal stresses in the slope. The maximum value appears in region B with 23.95 MPa. The contour of the figure shows the plastic strain with a maximum value of 608 $\mu\varepsilon$. The greatest stresses were experienced at the location of the ore pillar in area B, and plastic deformation occurred. In Figure 6(c), it can be seen that blast vibration again causes the redistribution of internal stresses in the slope. The von Mises stress maximum occurred in the B region and varied with blasting time, as shown in Figure 6(d). Taking the calculated stress response into account in the second step, the maximum value was 23.95 MPa at 0 s. When the blasting finished at 0.76 s, the maximum value was 23.41 MPa. The peak maximum value was 24.09 MPa which happened at 0.095 s. The contour lines in Figure 6 (c) are plastic strain, located in the pillar at point B, and the maximum value is 47.6 $\mu\varepsilon$. Compared with the stresses after hanging-wall ore mining, the stress distribution pattern of the slope after open-pit blasting is not much different.

In order to analyze the effect of open blasting on the slope surface, the variation of von Mises stress on the slope surface was calculated. The red line in Figure 7(a) shows the slope surface, where points A, B, C, and D are the locations of the foot of the slope immediately adjacent to the hanging-wall ore. We assume that the horizontal coordinate of the location of the lowest foot of the slope is 0. Figure 7(b) shows the variation of von Mises stress on the slope surface at 0 s, 0.25 s, 0.5 s, and 0.76 s after open blasting. The figure shows that the stresses on the slope surface at different times after blasting are similar in magnitude and have the same change pattern. The larger values of stress are concentrated at the location of the foot of the slope immediately adjacent to the hanging-wall ore. Its maximum value is 20.39 MPa, which occurs at 0 s of open-pit blasting. Figure 7(c) shows the variation law of von mises stress in four points A, B, C, and D under the action of blast vibration wave. In Figure 7 (c), it can be seen that among the four points, the stress at point C is the largest, 18.5 MPa at 0 s and 12.9 MPa at 0.76 s. The remaining points also showed different degrees of reduction, with point A decreasing from 10.8 MPa to 7.6 MPa, point B decreasing from 13.1 MPa to 9.3 MPa, and point D decreasing from 7.6 MPa to 5.5 MPa. The pillar of the slope adjacent to the hanging-wall ore is the security pillar, which is the weak link in the whole hanging-wall ore slope system. The surface of the security pillar has the highest force among the whole slope surface after hanging-wall ore mining. As shown in Figure 7(c), the stress distribution pattern of the slope surface after open-pit blasting is not significantly different compared with the stress after hanging gang mining. This indicates that open-pit blasting did not increase the stresses on the slope surface of the security pillar.

3.2.2. Comparative Analysis of Vibration Speed. The combined vibration velocity of each moment could be collected after open-pit blasting by numerical simulation. Results show that the combined vibration velocity of the slope reached its maximum value when $t = 0.265$ s. The contour plot of the combined vibration velocity is shown in Figure 8(a). The combined vibration velocity of the slope surface reaches the maximum at $t = 0.325$ s. The contour plot of its combined vibration velocity is shown in Figure 8 (b).

As can be seen in Figure 8(a), the peak vibration velocity is located in the first row of the hanging-wall ore column,

with a maximum value of about 7.40 cm/s. In Figure 8(b), it can be seen that the peak vibration velocity is located near position D and the maximum value is about 6.97 cm/s. According to *the blasting safety regulations*, when the main vibration frequency is greater than 10 Hz and less than 50 Hz, the safe allowable mass vibration velocity range for the mine tunnel is 18–25 cm/s. The safe allowable mass vibration velocity range for permanent rocky high slopes is 8 to 12 cm/s. It can be seen that the maximum peak value of particle vibration velocity of the slope under open blasting vibration is less than the safe allowable value of particle vibration velocity of the slope. It indicates that the current blasting vibration has little effect on this slope, which is stable under the joint action of dynamic and static loads.

4. Conclusions

According to the test data of blasting vibration wave monitoring on site, Sodev's formula was used to fit the blasting vibration propagation law of the east slope. The results of numerical simulation analysis showed that the current blasting vibration had little effect on this slope and the slope was stable under the combined action of dynamic and static loads. This can be used as the basis for predicting the maximum single-segment dose and minimum safe distance at this site.

It should be noted that in this paper, the focus was on the effect of open-pit blasting on the east slope of the Beizhan iron ore mine, ignoring the freeze-thaw action on the slope surface, anisotropy, and nonuniformity of the actual rock mass. We will take these factors into account for the next step of our research. The research methods and conclusions of this paper are good references for studying the dynamic stability of slopes with hanging-wall ore mines.

Data Availability

This study was approved and assisted by Hejing County Beizhan Mining Co. Ltd. The data used to support the findings of this study are included in the article.

Conflicts of Interest

The authors declare that they have no conflicts of interest regarding the publication of this paper.

Acknowledgments

This study was financially supported by the National Key R&D Program of China (Grant no. 2018YFC0808402). This financial support is gratefully acknowledged. Thanks are due to Hejing County Beizhan Mining Co. Ltd for the convenient conditions for blasting vibration detections.

References

[1] D. Q. Li, S. H. Jiang, Z. J. Cao, C. B. Zhou, X. Y. Li, and L. M. Zhang, "Efficient 3-D reliability analysis of the 530 m high abutment slope at Jinping I Hydropower Station during construction," *Engineering Geology*, vol. 195, pp. 269–281, 2015.

[2] C. A. Tang, L. C. Li, N. W. Xu, and K. Ma, "Microseismic monitoring and numerical simulation on the stability of high- steep rock slopes in hydropower engineering," *Journal of Rock Mechanics and Geotechnical Engineering*, vol. 7, no. 5, pp. 493–508, 2015.

[3] Y. K. Chen, J. H. Xu, X. H. Huo, and J. C. Wang, "Numerical simulation of dynamic damage and stability of a bedding rock slope under blasting load," *Shock and Vibration*, vol. 2019, 13 pages, 2019.

[4] B. H. Tan, F. Y. Ren, Y. J. Ning, R. X. He, and Q. Zhu, "A new mining scheme for hanging-wall ore-body during the transition from open pit to underground mining: a numerical study," *Advances in Civil Engineering*, vol. 2018, 17 pages, 2018.

[5] P. K. Singh, M. P. Roy, and R. K. Paswan, "Controlled blasting for long term stability of pit-walls," *International Journal of Rock Mechanics and Mining Sciences*, vol. 70, pp. 388–399, 2014.

[6] Y. G. Hu, M. S. Liu, X. X. Wu, G. Zhao, and P. Li, "Damage-vibration couple control of rock mass blasting for high rock slopes," *International Journal of Rock Mechanics and Mining Sciences*, vol. 103, pp. 137–144, 2018.

[7] Z. Q. Yin, Z. X. Hu, Z. D. Wei et al., "Assessment of blasting-induced ground vibration in an open-pit mine under different rock properties," *Advances in Civil Engineering*, vol. 2018, 10 pages, 2018.

[8] P. Rajmeny and R. Shrimali, "Use of radar technology to establish threshold values of blast vibrations triggering sliding of geological faults at a lead-zinc open pit mine," *International Journal of Rock Mechanics and Mining Sciences*, vol. 113, pp. 142–149, 2019.

[9] Z. Tao, C. Zhu, X. Zheng, and M. He, "Slope stability evaluation and monitoring of Tonglushan ancient copper mine relics," *Advances in Mechanical Engineering*, vol. 10, no. 8, 2018.

[10] D. R. Bao, Y. T. Gao, S. Xiao, and G. Kong, "Monitoring of blasting vibration and numerical simulation of a foreign open-pit mine slope," *Modern Mining*, vol. 12, pp. 121–125, 2015.

[11] C. Y. Xie, Z. Q. Luo, N. Jia, L. X. Xiong, and G. H. Cheng, "Dynamic effects of open blasting vibration on adjacent buildings and measures for vibration reduction," *Journal of Vibration & Shock*, vol. 32, no. 13, pp. 187–192, 2013.

[12] L. Ma, K. M. Li, S. S. Xiao, X. H. Ding, and S. Chordata, "Research on effects of blast casting vibration and vibration absorption of presplitting blasting in open cast mine," *Shock and Vibration*, vol. 2016, 9 pages, 2016.

[13] J. Hu, Y. Luo, and J. Xu, "Experimental and numerical analysis and prediction of ground vibrations due to heavy haul railway viaduct," *Mathematical Problems in Engineering*, vol. 2019, 15 pages, 2019.

[14] H. Ma, Y. Long, X. Li, M. Zhong, Q. Yin, and Q. Xie, "Attenuation and time-frequency characteristics of explosion ground vibration of shallow buried od1422-x80mm-12 MPa pipeline based on prototype experiment," *Journal of Performance of Constructed Facilities*, vol. 34, pp. 1–12, 2020.

[15] W. Gu, Z. Wang, J. Liu, J. Xu, X. Liu, and T. Cao, "Water-depth-based prediction formula for the blasting vibration velocity of lighthouse caused by underwater drilling blasting," *Shock and Vibration*, vol. 2017, 9 pages, 2017.

[16] Y. G. Hu, W. B. Lu, M. Chen, P. Yan, and J. H. Yang, "Comparison of blast-induced damage between presplit and smooth

blasting of high rock slope," *Rock Mechanics and Rock Engineering*, vol. 47, no. 4, pp. 1307–1320, 2014.

[17] N. Jiang, C. B. Zhou, S. W. Lu, and Z. Zhang, "Effect of underground mine blast vibrations on overlaying open pit slopes: a case study for daye iron mine in China," *Geotechnical and Geological Engineering*, vol. 36, no. 3, pp. 1475–1489, 2017.

[18] Y. T. Yang, G. H. Sun, H. Zheng, and Y. Qi, "Investigation of the sequential excavation of a soil-rock-mixture slope using the numerical manifold method," *Engineering Geology*, vol. 256, pp. 93–109, 2019.

[19] T. Bhandari, F. Hamad, C. Moormann, K. G. Sharma, and B. Westrich, "Numerical modelling of seismic slope failure using MPM," *Computers and Geotechnics*, vol. 75, pp. 126–134, 2016.

[20] M. Yilmaz, A. Ertin, S. Er, and A. Tugrul, "Numerical modelling of steep slopes in open rock quarries," *Journal of the Geological Society of India*, vol. 91, no. 2, pp. 232–238, 2018.

[21] Z. G. Qian, A. J. Li, A. V. Lyamin, and C. C. Wang, "Parametric studies of disturbed rock slope stability based on finite element limit analysis methods," *Computers and Geotechnics*, vol. 81, pp. 155–166, 2017.

[22] N. Jiang, C. B. Zhou, S. W. Lu, and Z. Zhang, "Propagation and prediction of blasting vibration on slope in an open pit during underground mining," *Tunnelling and Underground Space Technology*, vol. 70, pp. 409–421, 2017.

[23] N. Babanouri, H. Mansouri, S. K. Nasab, and M. Bahaadini, "A coupled method to study blast wave propagation in fractured rock masses and estimate unknown properties," *Computers and Geotechnics*, vol. 49, pp. 134–142, 2013.

[24] N. X. Xu, J. Y. Zhang, H. Tian, G. Mei, and Q. Ge, "Discrete element modeling of strata and surface movement induced by mining under open-pit final slope," *International Journal of Rock Mechanics and Mining Sciences*, vol. 88, pp. 61–76, 2016.

[25] H. Y. Liu, Y. M. Kang, and P. Lin, "Hybrid finite–discrete element modeling of geomaterials fracture and fragment muckpiling," *International Journal of Geotechnical Engineering*, vol. 9, no. 2, pp. 115–131, 2015.

[26] A. Haghnejad, K. Ahangari, P. Moarefvand, and K. Goshtasbi, "Numerical investigation of the impact of rock mass properties on propagation of ground vibration," *Natural Hazards*, vol. 96, no. 2, pp. 587–606, 2019.

[27] Z. Song, H. Konietzky, and M. Herbst, "Drawing mechanism of fractured top coal in longwall top coal caving," *International Journal of Rock Mechanics and Mining Sciences*, vol. 130, p. 104329, 2020.

[28] W. X. Li, D. L. Qi, S. F. Zheng, J. C. Ren, J. F. Li, and X. Yin, "Fuzzy mathematics model and its numerical method of stability analysis on rock slope of opencast metal mine," *Applied Mathematical Modelling*, vol. 39, no. 7, pp. 1784–1793, 2015.

[29] Y. Q. Liu, X. R. Liu, Y. M. Lu, X. W. Li, and P. Li, "Numerical analysis of evaluation methods and influencing factors for dynamic stability of bedding rock slope," *Journal of Vibroengineering*, vol. 19, no. 3, pp. 1937–1961, 2017.

[30] Z. Zhang, J. Han, and G. B. Ye, "Numerical investigation on factors for deep-seated slope stability of stone column-supported embankments over soft clay," *Engineering Geology*, vol. 168, pp. 104–113, 2014.

[31] I. Mehdipour, M. Ghazavi, and R. Z. Moayed, "Numerical study on stability analysis of geocell reinforced slopes by considering the bending effect," *Geotextiles and Geomembranes*, vol. 37, pp. 23–34, 2013.

[32] X. Y. Li, L. M. Zhang, and S. H. Jiang, "Updating performance of high rock slopes by combining incremental time-series monitoring data and three-dimensional numerical analysis," *International Journal of Rock Mechanics and Mining Sciences*, vol. 83, pp. 252–261, 2016.

[33] Y. Hu, Z. Yang, S. Huang, W. Lu, and G. Zhao, "A new safety control method of blasting excavation in high rock slope with joints," *Rock Mechanics and Rock Engineering*, vol. 53, no. 7, pp. 3015–3029, 2020.

[34] Y. Hu, W. Lu, M. Chen, P. Yan, and Y. Zhang, "Numerical simulation of the complete rock blasting response by sph-dam-fem approach," *Simulation Modelling Practice and Theory*, vol. 56, pp. 55–68, 2015.

[35] N. Jiang, T. Gao, C. Zhou, and X. Luo, "Effect of excavation blasting vibration on adjacent buried gas pipeline in a metro tunnel," *Tunnelling and Underground Space Technology*, vol. 81, pp. 590–601, 2018.

[36] H. R. Mohammadi Azizabadi, H. Mansouri, and O. Fouché, "Coupling of two methods, waveform superposition and numerical, to model blast vibration effect on slope stability in jointed rock masses," *Computers and Geotechnics*, vol. 61, pp. 42–49, 2014.